Polyimide-Polydimethylsiloxane Copolymers. Evaluation of the Thermal and Electrical Properties

Elena Hamciuc[a]; Corneliu Hamciuc[a]; Maria Cazacu[a]; Gabriela Lisa[b]; Lidia Okrasa[c]
[a] "Petru Poni" Institute of Macromolecular Chemistry, Iasi, Romania [b] Faculty of Industrial Chemistry, "Gh. Asachi" Technical University, Iasi, Romania [c] Department of Molecular Physics, Technical University of Lodz, Lodz, Poland

PLEASE SCROLL DOWN FOR ARTICLE

Polyimide-Polydimethylsiloxane Copolymers. Evaluation of the Thermal and Electrical Properties

ELENA HAMCIUC,[1] CORNELIU HAMCIUC,[1] MARIA CAZACU,[1] GABRIELA LISA,[2] and LIDIA OKRASA[3]

[1] *"Petru Poni" Institute of Macromolecular Chemistry, Iasi, Romania*
[2] *Faculty of Industrial Chemistry, "Gh. Asachi" Technical University, Iasi, Romania*
[3] *Department of Molecular Physics, Technical University of Lodz, Lodz, Poland*

Poly(dimethylsiloxane-amic-acid)s have been prepared starting from a fluorinated dianhydride, namely 4,4′-(hexafluoroisopropylidene)-diphthalic anhydride, and a mixture of an aromatic diamine and bis(aminopropyl)-oligodimethylsiloxane of controlled molecular weight, in different ratios. A solution imidization procedure was used to convert them quantitatively to the corresponding polyimides. The polymers, easily soluble both in polar (N-methylpyrrolidone) and less polar (chloroform) solvents, were prepared for film-forming by casting from solution. The thermal behavior in dependence on composition was evaluated by thermogravimetric analysis and differential scanning calorimetry. The kinetic processing of thermogravimetric data was carried out using the Flynn-Wall-Ozawa and Kissinger methods. Electrical insulating properties of some polymer films were evaluated on the basis of dielectric constant and dielectric loss tangent and their variation with frequency.

Keywords: polyimide-polydimethylsiloxane copolymers; good solubility; thermal stability; thermal degradation kinetics; thin films; dielectric constant

1 Introduction

High performance polymers are used in applications demanding service at enhanced temperatures while maintaining their structural integrity and an excellent combination of chemical, physical and mechanical properties. Wholly aromatic polyimides are generally the polymers of choice for these applications due to their many desirable characteristics including good thermooxidative stability and excellent mechanical properties (1–3). However, aromatic polyimides are often insoluble in their fully imidized form, presenting serious processing difficulties. Conventional aromatic polyimides must be processed at their precursor stage, poly(amic-acid)s, which are unstable at room temperature and must be stored at a lower temperature. The imidization process should be carried out in the final materials, at high temperature (250–300°C). This process has some inherent limitations like the generation of water, which would create voids in those materials (4). To overcome these problems, much research effort has been focused on the synthesis of soluble polyimides

in fully imidized form, without deterioration of their own excellent properties (5–7). In this respect, the incorporation of flexible polydimethylsiloxane segments into the polyimide backbone can yield soluble, processable copolyimides with good thermomechanical properties. The polydimethylsiloxane component imparts a number of beneficial properties to the polymeric system into which it is co-reacted, including enhanced solubility, reduced water absorption and gas permeability, good thermal and ultraviolet stability, resistance to degradation and modified surface properties. Also, the introduction of non-polar monomers results in polyimide systems with lower dielectric constant than classical aromatic polyimides (8–15).

The incorporation of hexafluoroisopropylidene (6F) groups into polymer backbones enhances the polymer solubility without sacrificing thermal stability. Other effects of the 6F groups are the increased glass transition temperature and flame resistance with a concomitant decreased water absorption. The bulky 6F groups also serve to increase the free volume of the polymers, thus improving its electrical insulating characteristics (16–20).

In this article, we present the synthesis of copolyimides containing polydimethylsiloxane sequences and 6F units. The properties of these polymers such as solubility, inherent viscosity, thermal stability, glass transition temperature and

Address correspondence to: Elena Hamciuc, "Petru Poni" Institute of Macromolecular Chemistry, Aleea Grigore Ghica Voda 41A, Iasi 700487, Romania. E-mail: ehamciuc@icmpp.ro

electrical characteristics of the polymer films made from these compounds, have been evaluated with respect to their chemical structure. The thermostability was evaluated based on the thermal characteristics out of thermogravimetric data. The kinetic data processing was performed by applying Flyn-Wall-Ozawa (21, 22) and Kissinger (23) methods, following the influence of the heating rate and the dependency activation energy-conversion degree.

2   Experimental

2.1   Synthesis of the Monomers

α,ω-Bis(aminopropyl)oligodimethylsiloxane **3** was synthesized by anionic polymerization of octamethylcyclotetrasiloxane in the presence of tetramethylamonium hydroxide as a catalyst and 1,3-bis(aminopropyl)tetramethyldisiloxane as an end-blocker (24). An oligomer with molar mass of 750 g/mol estimated by ^{1}H-NMR spectroscopy was obtained by choosing a proper ratio between cyclic monomer and end-blocker (2:1 molar).

The other monomers like 4,4′-(hexafluoroisopropylidene)-diphthalic anhydride, **1**, and bis(*p*-aminophenoxy)-4,4′-biphenyl, **2**, have been obtained from commercial sources and used as received.

2.2   Synthesis of the Polymers

The non-siloxane containing poly(amic acid) intermediate **4a** was synthesized by slowly adding the solid dianhydride **1** to a stirring solution of the diamine **2**. The reaction was conducted at room temperature, under a nitrogen atmosphere, in N-methylpyrrolidone (NMP). The polymer solution was heated at 180–185°C for 4 h under a nitrogen stream, to perform the cyclization of the poly(amic-acid) **4a** to the corresponding polyimide structure **5a**, according to a method previously described (25).

The polydimethylsiloxane-containing poly(amic-acid) intermediates **4b** and **4c** were obtained as is described in the following example. To a solution of the dianhydride **1** (0.888 g, 2 mmol) in 6 ml of NMP/tetrahydrofuran (THF) (1:1), an amine-terminated oligodimethylsiloxane **3** (0.595 g, 0.8 mmol) solution in 4 ml of THF was slowly added at room temperature. After the mixture was stirred for 1 h, diamine **2** (0.441 g, 1.2 mmol) in 6 ml NMP was added, and the mixture was stirred at room temperature for 10 h. The yellow, viscous solution was imidized by heating in a mixture of *m*-xylene-NMP (2/5, v/v) at reflux temperature, for 4 h, at a concentration of 10%. The xylene was distilled off under vacuum and the resulting solution was precipitated in a large quantity of water to give a yellow-brown rubbery material, **5b**, which was dried in vacuum at 80°C, for 24 h. The yield of the reaction was 85%. The synthesis of poly(amic-acid)s **4** and polyimides **5** is presented in Scheme 1.

2.3   Preparation of Polymer Films

Films of polymer **5a** were prepared by using a 10% polymer solution in NMP, which was cast onto glass plates and dried gradually at 100°C, 130°C, 160°C, 190°C, and 220°C, each for 30 min. The resulting flexible transparent films were stripped off the plates by immersion in hot water for 2 h. Films of polymers **5b** and **5c** were similarly prepared by casting a solution of 5% concentration of polymer in chloroform onto glass plates, followed by drying at room temperature for 24 h under a Petri dish and for another 2 h at 130°C (26).

2.4   Measurements

Melting points of the monomers and intermediates were measured on a Melt-Temp II (Laboratory Devices).

The inherent viscosities (η_{inh}) of the polymers were determined with an Ubbelohde viscometer, by using polymer solutions in NMP, at 20°C, at a concentration of 0.5 g/dL.

Infrared spectra were recorded with a Specord M80 spectrometer by using KBr pellets.

^{1}H-NMR spectra were recorded using an Avance DRXx400, at room temperature. The glass transition temperature (T_g) of the precipitated polymers was determined with a Mettler differential scanning calorimeter (DSC 12E), at a heating rate of 10°C/min, under nitrogen. Heat flow vs. temperature scans from the second heating run were plotted and used for reporting the glass transition temperature. The mid-point of the inflexion curve resulting from the typical second heating was assigned as the glass transition temperature of the respective polymers.

The dynamic mechanical analysis (DMA) was conducted using a Perkin−Elmer Diamond apparatus provided with a standard tension attachment at a frequency of 1 Hz. The apparatus was heated between −150°C and 200°C at 2°C/min, in a nitrogen atmosphere. The films (20 × 10 × 0.5 mm) were longitudinally deformed by small sinusoidal stress and the resulting strain was measured. The value of storage modulus E', the loss modulus E'' and tension loss tangent (*tan* $\delta = E''/E'$) were obtained as a function of temperature.

Thermogravimetric analysis (TGA) was performed under nitrogen flow (15 cm^3/min) at various heating rates 7°C/min, 10°C/min, 15°C/min and 20°C/min from 25°C to 900°C with a Mettler Toledo model TGA/SDTA 851. The initial mass of the samples was 4-6 mg.

The analysis of the dielectric properties has been performed in a parallel plate capacitor under a sinusoidal voltage. Solid samples in the form of films having thickness of 25 μm with evaporated golden electrodes (10 mm diameter) have been examined. The frequency analyzer Solartron Schlumberger 1260 (10^{-1}–10^6 Hz) has been used. The complex dielectric permittivity (ε^*), given by the equation $\varepsilon^* = \varepsilon' + \varepsilon''$, where ε' is the real component of the dielectric constant and ε'' is the imaginary component of the dielectric constant, has been measured as a function
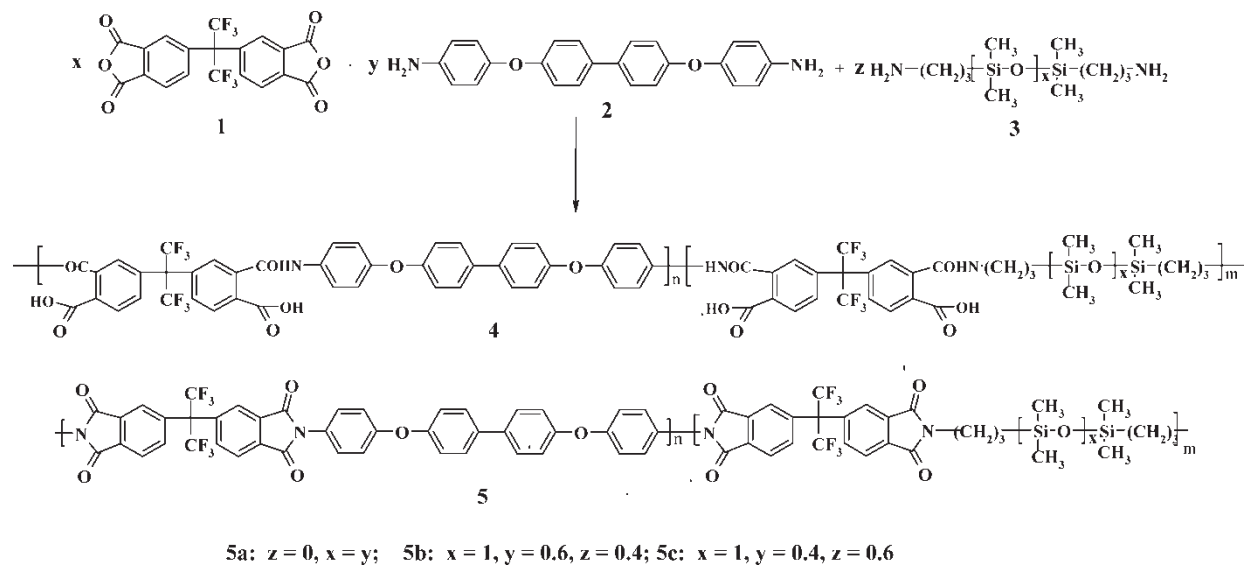
Sch. 1. Preparation of poly(amic acid)s **4** and polyimides **5**.

3 Results and Discussion

3.1 Synthesis Procedure

The synthesis of aromatic polyimide **5a** took place in two steps, in one pot. In the first step, the polycondensation of aromatic diamine **2** with aromatic dianhydride **1** was performed at room temperature, under nitrogen, leading to the poly(amic acid) **4a** (Scheme 1).

In the second step, the resulting solution of poly(amic-acid) **4a** was heated, at $180-185°C$, for 4 h, to give the polyimide **5a**. The water of imidization was evacuated by a slow stream of nitrogen which was used as inert medium, at the same time.

The polydimethylsiloxane-containing poly(amic acid)s **4b** and **4c** (Scheme 1) were synthesized by a slightly different method. A co-solvent system consisting of NMP and THF was necessary to acomplish homogeneous solution copolymerization. The siloxane oligomer **3** was first added to a solution of the diahydride **1**. The aromatic diamine **2** was then gradually added as a solution in NMP to the free dianhydride and anhydride capped polydimethylsiloxane. The cyclization of the poly(amic acid)s **4b** and **4c** to the corresponding polyimide structures **5b** and **5c** was performed in a mixture of *m*-xylene/NMP, at reflux temperature.

3.2 Chemical Structure and General Characterization

The conversion of poly(amic-acid)s **4** to the fully cyclized polyimides **5** was confirmed by IR spectroscopy. The complete conversion of *o*-carboxy-amide groups to the imide ring was evidenced by the disappearance of the amic bands at $1650-1700$ cm^{-1} and $2500-3000$ cm^{-1}. In all, IR spectra of polymers **5** strong bands appearing at $1780-1770$ cm^{-1} and $1720-1710$ cm^{-1} were assigned to symmetrical and asymmetrical stretching vibrations of carbonyl groups of imide rings. Absorption band at 1380 cm^{-1} was due to C-N stretching of imide rings, and absorption band at 720 cm^{-1} is assigned to imide ring deformation. The absorption peak at 1240 cm^{-1} is assigned to the aromatic ether Ar-O-Ar. Aromatic C=C bands were found at 1600 cm^{-1} and 1500 cm^{-1}. All the polymers **4** and **5** showed characteristic absorption bands at 1180 cm^{-1} and 1210 cm^{-1} due to 6F groups. In the IR spectra of polymers **4b**, **4c**, **5b**, and **5c** the presence of siloxane units was evidenced by the characteristic absorption bands at 2980 cm^{-1} due to the methyl groups, at 1080 cm^{-1} (Si-O-Si) and 800 cm^{-1} (H$_3$C-Si). Figure 1 shows the IR spectra of poly(amic acid) **4b** and the corresponding polyimide **5b**, as an example.

Figure 2 presents the ^{1}H-NMR spectrum of the polymer **5b** with the assignments of all the protons. The protons H_a, H_b and H_c closed to the imide ring appeared at the farthest downfield region of the spectrum. The protons H_e and H_f shifted to a higher field due to the electron donating properties of aromatic ether. The imidization of the poly(amic acid)s was also confirmed by the fact that ^{1}H-NMR spectra of polymers **5** showed no residual resonance in the region $9-11$ ppm indicating the absence of amide NH protons. The ^{1}H-NMR spectra of polymers **5b** and **5c** showed a characteristic peak at 3.65 ppm corresponding to methylene group adjacent to the terminated imide function. The characteristic peaks corresponding to the protons H_k and H_m appeared at 1.7 ppm and 0.57 ppm, respectively. The protons of methyl groups from the polydimethylsiloxane segments appeared at 0.05 ppm.

Of frequency at constant temperature. The dielectric loss tangent is defined by $tan\delta = \varepsilon''/\varepsilon'$ and was determined as a function of frequency.
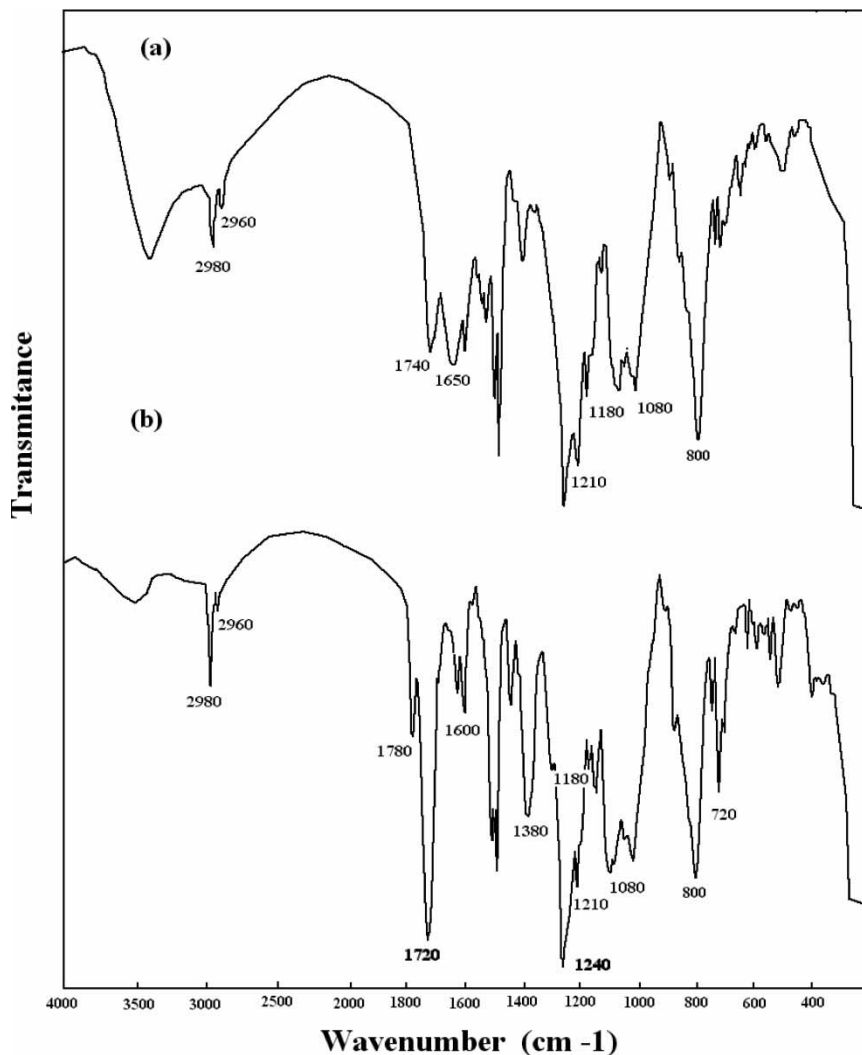
Fig. 1. IR spectra of poly(amic acid) **4b** (a) and corresponding polyimide **5b** (b).

The polyimide **5a** was soluble in aprotic solvents such as NMP, N,N-dimethylacetamide or N,N-dimethylformamide. The good solubility allowed the imidization process to be performed in solution so that the final polymer was obtained as an imidized product, which is more convenient than using poly(amic acid). The good solubility of the present polyimide is explained by the presence of flexible bridges such as ether and 6F, which disturb the packing of the polymer and make the shape of the respective macromolecule to be far from a linear rigid rod that is characteristic to conventional polyimides. The polymers **5b** and **5c** were soluble in polar solvents like NMP and even in less polar solvents like chloroform. The higher solubility of these polymers on compared with non-siloxane polyimide **5a**, can be explained by the presence of flexible polydimethylsiloxane segments which improve the flexibility of the macromolecular chains thus improving the solubility.

The inherent viscosity of the polymers was in the range of 0.32–0.71 dL/g (Table 1).

All polyimides exhibited film-forming ability. In the case of polymer **5a**, NMP was used as solvent for the preparation of films, while in the case of polymers **5b** and **5c** chloroform was used as solvent. The polymer solutions were cast onto glass substrates and dried to yield free standing films having a thickness of 20–30 μm. The films obtained from polymer **5c**, having a higher concentration of polydimethylsiloxane segments, were brittle.

3.3 Thermal Properties

The upper glass transition temperature (T_g) of the polyimides **5**, evaluated from DSC curves, was in the range of 155–215°C. The DSC measurements showed no evidence of crystallization or melting which proves an amorphous morphology. A decrease of T_g by increasing the concentration of the polydimethylsiloxane segments into the macromolecular chain of polyimide was observed. Thus, the polymer **5c**,
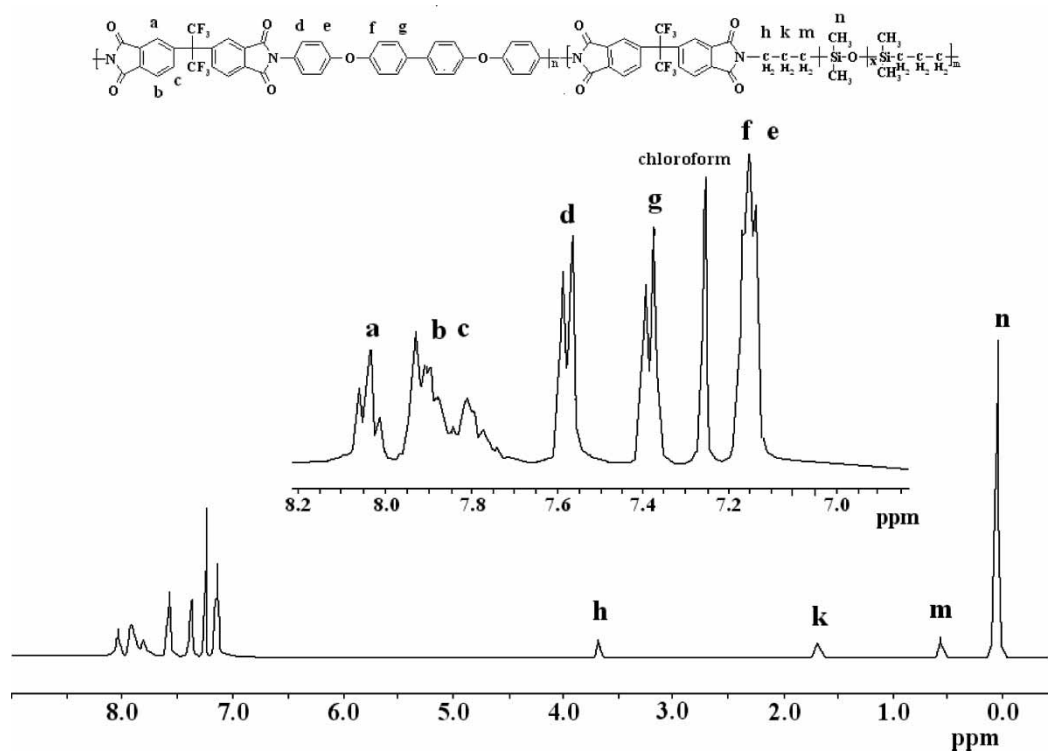
Fig. 2. ^{1}H-NMR spectrum of polymer **5b**.

having the highest concentration of polydimethylsiloxane segments, exhibited the lowest T_g (155°C) (Table 1).

Dynamic mechanical analysis (DMA) is generally more sensitive than calorimetric methods and can provide a relatively good definition of T_g. Figure 3 presents the temperature dependence of the storage modulus (E'), loss modulus (E'') and loss tangent (*tan δ*) for polymer **5b**. This polymer shows two different transitions due to polydimethylsiloxane and imide segments characteristic of a thermoplastic elastomer. The high-temperature transition is attributed to the polyimide phase. The T_g value of polymer **5b** is 175°C and is lower than that of polymer **5a** (230°C) because the average sequence length of the hard segments is expected to be shorter than it would be the corresponding polymer without polydimethylsiloxane segments (Table 1). At low temperatures the polymer **5b** has a T_g of -108°C. Thus, in this

region it can be observed that the storage modulus E' drops and appeared a peak for *tan δ*.

The thermal stability of the polymers was evaluated by dynamic thermogravimetric analysis in nitrogen gas, at four different heating rates. Figures 4 and 5 show the TG and the differential weight loss (DTG) curves of the polymers **5**, with the heating rate of 15°C/min.

The summary of the important thermogravimetric characteristics obtained from the thermograms are listed in Table 2 at the different heating rates for the polymers **5**. All polymers exhibited high thermal stability, with insignificant weight loss up 420°C. They began to decompose in the range of 420−500°C, and the temperature of 10% weight loss ($T_{10\%}$) was in the range of 430−550°C (Table 2). A decrease of the thermal stability of polymers was observed by increasing the concentration of polydimethylsiloxane

Table 1. Properties of polymers **5**

| Polymer | $\eta_{inh}{}^a$(dL/g) | $T_g{}^b$(°C) | $T_g{}^c$(°C) | Dielectric constant at | | |
				100 Hz	10 kHz	1 MHz
5a	0.71	215	230	3.25	3.18	3.05
5b	0.48	175	186	3.03	3.00	2.95
5c	0.32	155	—	—	—	—

[a]Measured at a concentration of 0.5 g polymer in 100 mL of NMP, at 20°C.
[b]Glass transition temperature determined from DSC curve.
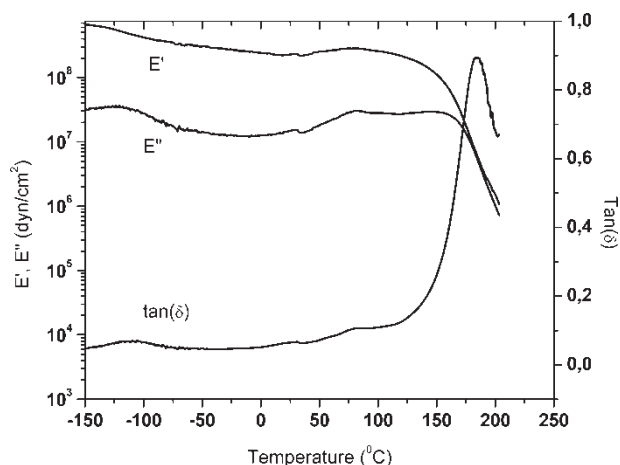[c]Glass transition temperature determined from DMA.

Fig. 3. DMA thermogram for polymer **5b**.

Fig. 5. DTG curves of polymers **5**, at 15°C/min.

segments. Thus, polymer **5c** having a higher content of poly-dimethylsiloxane exhibited the lowest thermal stability when compared with polymer **5a** not-containing polydimethylsiloxane segments.

Using as thermal stability criteria the onset temperature (T_{Onset}) for the polymer decomposition, the thermal stability series was established as being the following:

$$5c < 5b < 5a$$

The decrease of thermal stability of the polymers **5b** and **5c** can be explained by the lower thermal stability of polysiloxane segments when compared with that of the polyimide homopolymer **5a**. In the case of polysiloxane segments, the thermal degradation begins at the aliphatic *n*-propyl segments linking the siloxane oligomer to the polyimide matrix. Thus, as the content of polysiloxane oligomers is increased the concentration of *n*-propyl linkages in the copolymer backbone increases and the overall thermal stability is decreased (8). The same conclusion regarding the thermal stability is obtained even if the temperatures corresponding
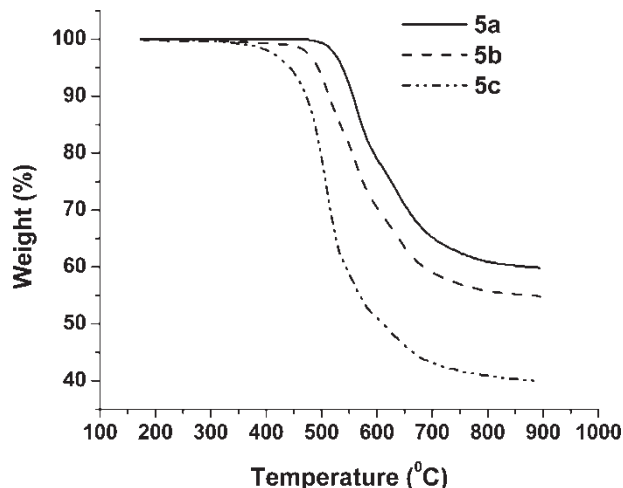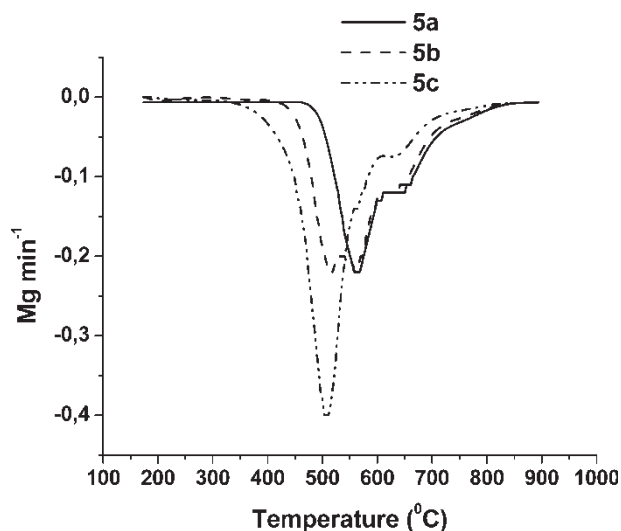
to 10%, 25% or 50% weight loss are considered as criteria of stability.

In order to explain the thermal degradation of the investigated materials, it is necessary to know the entire kinetic triplet (E_a, *ln A*, conversion function), not only the activation energy. The methods of calculating the activation energy (E_a) can be divided in two groups: multiple heating rate methods and single heating rate methods. As the multiple heating rate methods, Flynn-Wall-Ozawa and Kissinger methods were used. These two methods can be derived from a common fundamental kinetic equation for heterogeneous chemical reactions and therefore have common features, wide applicability and high reliability (27).

Flynn-Wall-Ozawa method is a relatively simple method of determining activation energy directly from weight loss vs. temperature data, obtained at several heating rates. The multiple heating-rate method proposed by Flynn-Wall-Ozawa uses the following approximate equation at a constant weight loss in a thermal degradation process:

$$\log a = \log \frac{A \cdot E_a}{R} - \log F(\alpha) - 2.315 - 0.4567 \frac{E_a}{RT} \quad (1)$$

where *a* is the heating rate in the TG measurement, *A*−pre-exponential factor, *R*−general gas constant (J/mol *K*), F(*α*)−conversional functional relationship and *T* is the absolute temperature (K). From this equation E_a can easily be calculated based on the slope of a plot of *log a* vs. *1/T* at a fixed weight loss. The Flynn-Wall-Ozawa method is the most useful method for the kinetic interpretation of the thermogravimetric data obtained when studying complex processes, like the thermal degradation of polymers. This method can determine the activation energy without knowledge of reaction order. In this work, the values of *ln A* are calculated from the intercept of the straight lines on the Y-axis (graph *log a* vs. *1/T*) for each conversion using the first reaction order kinetic model [$-ln(1 - \alpha)$]. The kinetic triplets (E_a,

Fig. 4. TG curves of polymers **5**, at 15°C/min.

Table 2. The thermogravimetrical parameters of polymers **5**

Polymer	The heating rate[a]	T_{Onset}[b](°C)	$T_{10\%}$[c](°C)	$T_{25\%}$[d](°C)	$T_{50\%}$[e](°C)	T_{End}[f](°C)	M_{Resid}[g](%)
5a	7	507.02	520.44	536.54	590.35	691.41	44.39
	10	515.83	540.56	540.56	602.75	721.32	42.40
	15	518.90	544.73	544.73	611.09	737.00	42.88
	20	527.19	553.32	553.32	617.84	747.51	41.56
5b	7	462.44	469.50	502.78	549.56	689.08	46.01
	10	474.29	481.84	508.80	555.27	694.91	45.93
	15	478.31	491.27	517.65	564.54	700.67	45.20
	20	489.28	499.16	526.21	571.49	713.23	44.92
5c	7	428.04	430.92	467.20	499.38	672.50	62.17
	10	439.93	441.41	480.30	515.59	698.85	62.47
	15	446.09	452.87	488.05	516.08	693.86	60.08
	20	451.33	460.51	494.96	521.15	691.99	60.38

[a]The heating rate at which thermogravimetric analyses were performed.
[b]The onset temperature of the polymer decomposition.
[c]Temperature corresponding to 10% weight loss.
[d]Temperature corresponding to 25% weight loss.
[e]Temperature corresponding to 50% weight loss.
[f]The end set temperatures of the polymer decomposition.
[g]Weight loss of the polymer after the end of the decomposition process.

ln A and conversion function) for polymers **5a**, **5b**, and **5c** are described in Table 3. It can be seen that the values of the average apparent energy of decomposition process decreased by increasing the polydimethylsiloxane content.

The Flynn-Wall-Ozawa diagrams (Figure 6 for polymer **5a** and Figure 7 for polymer **5b**) are characteristic to successive reactions, the line slope changing at certain conversion degrees.

The value of the activation energy for the thermal degradation of the polyimide-polydimethylsiloxanes was determined by the application of the Kissinger method that is based on the graphical representation $[ln\ a/T_{max}^2]$ depending on $[1/T_{max}]$ that is a line with the slope E_a/R and where a is the heating rate, and T_{max} is the temperature at which the degradation rate is the highest. The results obtained are presented in Table 4. The reaction order of the non-isothermal degradation process, n, has been determined by this method as being:

$$n = 1.26\sqrt{S} \qquad (2)$$

where S is the shape index of the differential thermal analysis curve for non-isothermal dynamic degradation. The shape index is the absolute value of ratio of slopes of tangents to the DTG curve at the inflection point, T_{max}. The reaction orders for degradation polymers **5** are shown in Table 4.

The results regarding the apparent activation energy obtained by both Flynn-Wall-Ozawa and Kissinger methods are approximately equal and confirm the series of thermal stability presented previously from thermogravimetric data, considering as criterion the onset temperatures (T_{Onset}) for the polymer decomposition (**5c** < **5b** < **5a**).

Table 3. The kinetic characteristics estimation by the Flynn-Wall-Ozawa method

Polymer	α[a]	E_a (kJ/mol)[b]	ln A[c]	r^2[d]
5a	0.1	244.59	34.70	0.997
	0.3	286.08	40.75	0.994
	0.5	243.61	34.55	0.983
	0.7	276.14	39.30	0.984
	0.9	307.12	43.82	0.915
	Average apparent activation energy[e]	271.50		
5b	0.1	162.37	24.25	0.991
	0.3	219.76	33.25	0.978
	0.5	238.80	36.24	0.994
	0.7	228.49	35.09	0.925
	0.9	201.24	30.35	0.930
	Average apparent activation energy[e]	210.13		
5c	0.1	144.08	21.80	0.999
	0.3	185.14	28.26	0.969
	0.5	210.97	32.33	0.945
	0.7	218.49	33.06	0.988
	0.9	128.79	19.40	0.975
	Average apparent activation energy[e]	177.49		

[a]The degree of conversion.
[b]Apparent activation energy.
[c]Pre-exponential factor.
[d]Correlation coefficients.
[e]E_a values summarized correspond to mean values obtained from different degrees of conversion.

To provide further evidence regarding the degradation system of the analyzed compounds, we studied the
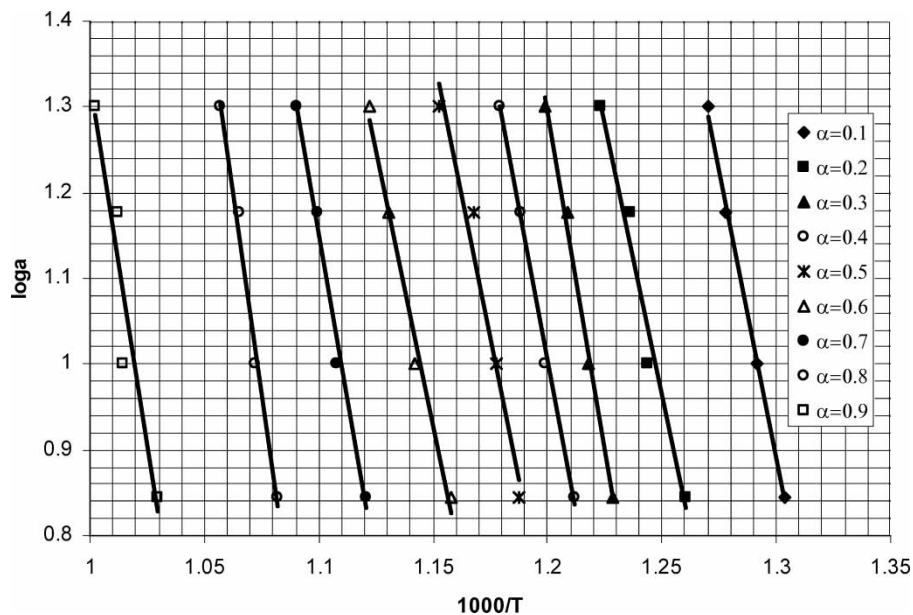
Fig. 6. Flynn-Wall-Ozawa diagrams for polymer **5a** (a-the heating rate; α-the conversion degree).
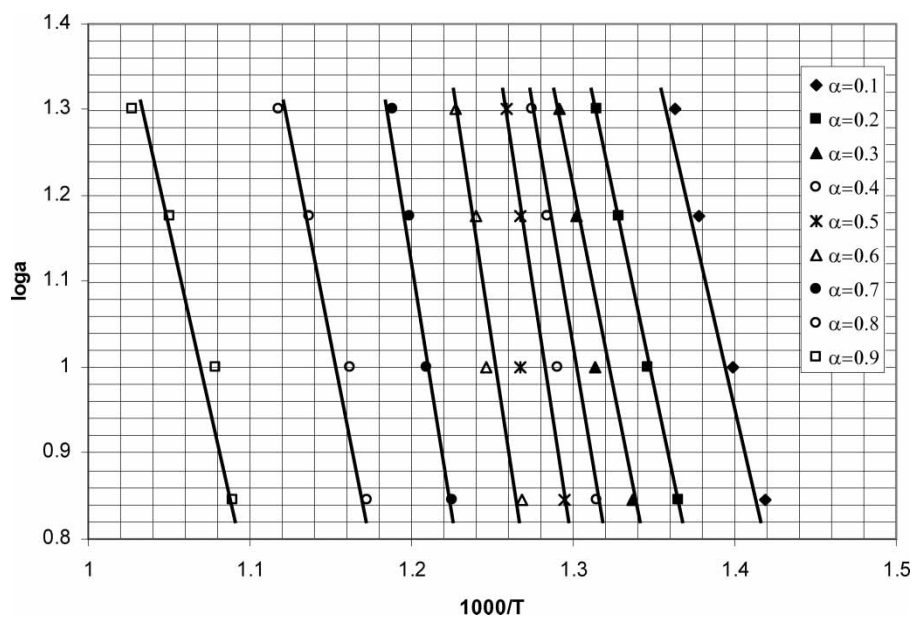

Fig. 7. Flynn-Wall-Ozawa diagrams for polymer **5b** (a-the heating rate; α-the conversion degree).

Table 4. The apparent activation energy values (E_a) estimation by the Kissinger method

Polymer	n^a	E_a (kJ/mol)^b	ln A^c	r^{2d}
5a	1.39	269.28	38.21	0.974
5b	1.70	199.95	29.05	0.993
5c	0.94	174.81	26.27	0.980

^{a}Reaction order.
^{b}Activation energy.
^{c}Pre-exponential factor.
^{d}Correlation coefficients.
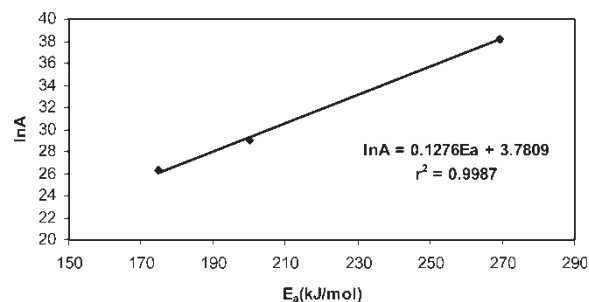

InA = 0.1276Ea + 3.7809
r^2 = 0.9987

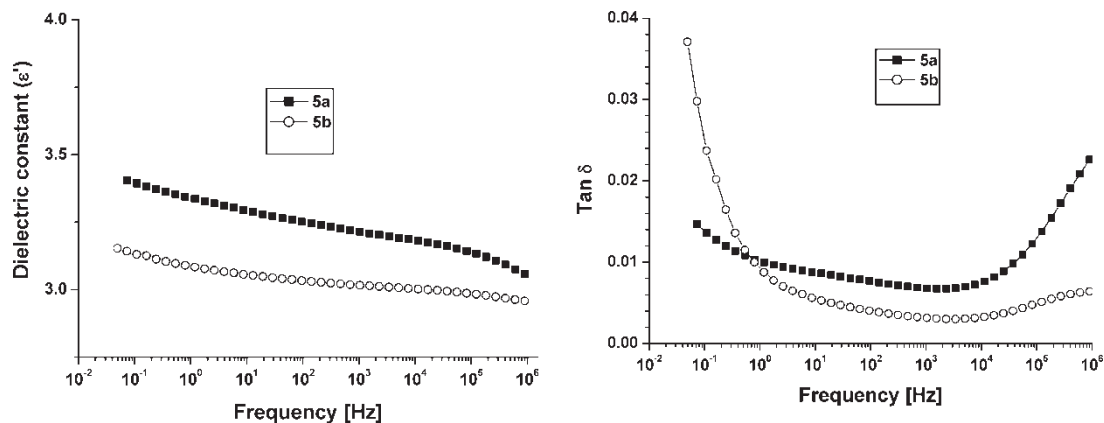**Fig. 8.** Compensation effect of the thermal degradation.

Fig. 9. Dielectric analysis plot showing the real dielectric constant and the dielectric loss tangent versus frequency, for polymers **5a** and **5b**.

compensation effect based on the kinetic parameters resulting by applying the Kissinger method (Table 4). Thus, we illustrated graphically the variation *ln A = f (E_a)* obtaining the compensation equation (Figure 8). The linear dependency confirms that the polymers exhibit a degradation mechanism similar, the line slope being about 0.12.

3.4 Dielectric Properties

Between the physical methods, which can be used to study polymers those involving the dielectric properties are very important. The electrical properties are required, when polymers are used for cable insulation, for capacitors, for insulation or packaging of electronic devices or as integral parts of electronic devices. Electrical insulating properties of polymer films **5a** and **5b** were evaluated on the basis of dielectric constant and dielectric loss tangent, and their variation with frequency.

The dielectric constant and dielectric loss tangent of polyimides **5a** and **5b** are displayed from 10^{-1}–10^{6} Hz. The dependence of both dielectric constant (ε') and dielectric loss tangent (*tan δ*) on frequency is shown in Figure 9.

The frequency dependencies are typical for the polymers. By increasing the frequency, a small monotonic decrease in ε' appeared. The dielectric loss tangent values are very small due to the very small values of ε'' of complex permittivity. The dielectric constants for the polymers at 100 Hz, 10 kHz and 1 MHz are listed in Table 1. The values at 10 kHz were in the 3.00–3.18 range. These values of the dielectric constant are even lower than that of "H Film", a polyimide which is prepared from pyromellitic dianhydride and 4,4′-diaminodiphenylether and which is one of the most preferred high performance dielectrics in microelectronic applications having a dielectric constant of 3.5 (2). This can be probably explained by the presence in the main chain of bulky 6F groups which increase free volume and thus lowering the polarization by decreasing the number of polarizable groups per unit volume. The polymer **5b** exhibited lower dielectric constant value due to the presence of hexafluorisopropylidene units and polydimethylsiloxane segments which increase the hydrofobicity, decrease the humidity absorption thus decreasing the dielectric constant.

4 Conclusions

Fluorinated polyimide-polydimethylsiloxane copolymers have been synthesized by solution polycondensation reaction of a mixture of an aromatic diamine and bis(amino-propyl) polydimethylsiloxane oligomer of controlled molecular weight with 4,4′-(hexafluoroisopropylidene)diphthalic anhydride. The introduction of siloxane oligomer into the macromolecular chain of an aromatic polyimide increases the solubility while decreasing the thermal stability, glass transition temperature and dielectric constant. The polymers are soluble in polar aprotic solvents and possess film forming ability. They show high thermal stability with decomposition temperature being in the range of 400–490°C and upper glass transition temperature in the range of 155–215°C. The thermal stability and degradation kinetics of these polymers have been reported in this work. Kinetic parameters of degradation were evaluated by using the Flynn-Wall-Ozawa and Kissinger methods. The thermal and kinetic characteristics enabled the determination of a series of analyzed polymers thermostability: **5c** < **5b** < **5a**. The polymer films exhibited low dielectric constant and low dielectric loss tangent in the interval of frequency 10^{-1}–10^{6} Hz.

5 Acknowledgements

6 References

1. Sillion, B. In *Comprehensive Polymer Science*; Allen, G. (ed.); Pergamon Press: Oxford; Vol. 5, 499–532, 1989.
2. Sroog, C.E. (1991) *Prog. Polym. Sci.*, **16**, 561–694.
3. Sato, M. Polyimides. In *Handbook of Thermoplastics*; Olabisi, O. (ed.); Marcel Dekker: New York; 665–669, 1997.
4. Hergenrother, P.M. (2003) *High Perform. Polym.*, **15**, 3–45.
5. Huang, S.J. and Hoyt, A.E. (1995) *Trends Polym. Sci.*, **3**, 262–271.
6. De Abajo, J. and de la Campa, J.G. (1999) *Adv. Polym. Sci.*, **140**, 23–59.
7. Yang, C.P., Hsiao, S.H. and Yang, C.C. (2004) *J. Polym. Research*, **11**, 23–29.
8. Arnold, C.A., Summers, J.D., Chen, Y.P., Bott, R.H., Chen, D. and McGrath, J.E. (1989) *Polymer*, **30**, 986–995.
9. Rogers, M.E., Glass, T.E., Mecham, S.J., Rodrigues, D., Wilkes, G.L. and McGrath, J.E. (1994) *J. Polym. Sci.: Part A: Polym. Chem.*, **32**, 2663–2675.
10. Furukawa, N., Yuasa, M. and Kimura, Y. (1998) *J. Polym. Sci.: Part A: Polym. Chem.*, **36**, 2237–2245.
11. Andre, S., Guida-Pietrasanta, F., Rousseau, A. and Boutevin, B. (2001) *J. Polym. Sci.: Part A: Polym. Chem.*, **39**, 2414–2425.
12. Takeichi, T., Agag, T. and Zeidam, R. (2001) *J. Polym. Sci.: Part A: Polym. Chem.*, **39**, 2633–2641.
13. Mahoney, C.M. and Gardella, J.A. Jr. (2002) *Macromolecules*, **35**, 5256–5266.
14. Racles, C., Cozan, V., Cazacu, M., Foldes, E. and Sajo, I. (2002) *High Perform. Polym.*, **14**, 397–413.
15. Simionescu, M., Sacarescu, L., Ardeleanu, R. and Sacarescu, G. (2005) *High Perform. Polym.*, **17**, 73–84.
16. Bruma, M., Fitch, J.W. and Cassidy, P.E. (1996) *J. Macromol. Sci.–Rev. Macromol. Chem. Phys.*, **C 36**, 119–159.
17. Hamciuc, C., Hamciuc, E., Bruma, M., Klapper, M. and Pakula, T. (2001) *Polym. Bull.*, **47**, 1–8.
18. Yang, C.P., Chen, R.S. and Chen, K.H. (2003) *J. Polym. Sci.: Part A: Polym. Chem.*, **41**, 922–938.
19. Hsiao, S.H. and Chen, W.T. (2003) *J. Polym. Research*, **10**, 95–103.
20. Hamciuc, C., Hamciuc, E. and Bruma, M. (2005) *Polymer*, **46**, 5851–5859.
21. Flynn, J.H. and Wall, L.A. (1966) *Polymer Letters*, **4**, 323–328.
22. Ozawa, T.A. (1965) *Bull. Chem. Soc. Jpn.*, **38**, 1881–1891.
23. Kissinger, H.E. (1957) *Anal. Chem.*, **29**, 1702–1712.
24. Cazacu, M., Vlad, A., Simionescu, M., Racles, C. and Marcu, M. (2002) *J. Macromol. Sci.-Pure and Appl. Chem.*, **39**, 1487–1499.
25. Hamciuc, E., Hamciuc, C., Bruma, M. and Schulz, B. (2005) *Eur. Polym. J,* **41**, 2989–2997.
26. Hamciuc, C., Hamciuc, E., Bruma, M., Klapper, M., Pakula, T. and Demeter, A. (2001) *Polymer*, **42**, 5955–5961.
27. Schneider, H.A. (1985) *Thermochim. Acta*, **83**, 59–70.